Effects of migration network configuration and migration synchrony on infection prevalence in geese

Yin, S.; Knegt, H.J. de; Jong, M.C.M. de; Si, Y.; Prins, H.H.T.; Huang, Z.Y.X.; Boer, W.F. de

Journal of Theoretical Biology 502 (2020) 110315

Contents lists available at ScienceDirect

Journal of Theoretical Biology

journal homepage: www.elsevier.com/locate/yjtbi

Effects of migration network configuration and migration synchrony on infection prevalence in geese

Shenglai Yin [b], Henrik J. de Knegt [b], Mart C.M. de Jong [c], Yali Si [d,e], Herbert H.T. Prins [b], Zheng Y.X. Huang [a,*], Willem F. de Boer [b]

[a] College of Life Science, Nanjing Normal University, 210046 Nanjing, China
[b] Wildlife Ecology and Conservation Group, Wageningen University, 6708PB Wageningen, The Netherlands
[c] Quantitative Veterinary Epidemiology Group, Wageningen University, 6708PB Wageningen, The Netherlands
[d] Institute for China Sustainable Urbanization, Tsinghua University, 100091 Beijing, China
[e] Institute of Environmental Sciences, Leiden University, 2300RA Leiden, Netherlands

ARTICLE INFO

Article history:
Received 5 December 2019
Revised 29 April 2020
Accepted 30 April 2020
Available online 5 May 2020

Keywords:
Avian influenza
Environmental transmission
Stopover site
Cumulative infection
SIR model

ABSTRACT

Migration can influence dynamics of pathogen-host interactions. However, it is not clearly known how migration pattern, in terms of the configuration of the migration network and the synchrony of migration, affects infection prevalence. We therefore applied a discrete-time SIR model, integrating environmental transmission and migration, to various migration networks, including networks with serial, parallel, or both serial and parallel stopover sites, and with various levels of migration synchrony. We applied the model to the infection of avian influenza virus in a migratory geese population. In a network with only serial stopover sites, increasing the number of stopover sites reduced infection prevalence, because with every new stopover site, the amount of virus in the environment was lower than that in the previous stopover site, thereby reducing the exposure of the migratory population. In a network with parallel stopover sites, both increasing the number and earlier appearance of the stopover sites led to an earlier peak of infection prevalence in the migratory population, because the migratory population is exposed to larger total amount of virus in the environment, speeding-up the infection accumulation. Furthermore, higher migration synchrony reduced the average number of cumulative infection, because the majority of the population can fly to a new stopover site where the amount of virus is still relatively low and has not been increased due to virus shedding of infected birds. Our simulations indicate that a migration pattern with multiple serial stopover sites and with highly synchronized migration reduces the infection prevalence.

1. Introduction

Many species migrate between their wintering and breeding grounds in response to seasonal changes in habitat conditions, such as food availability (Altizer et al., 2011; Dingle, 2014). Meanwhile, migration can also facilitate pathogen transmission, as migratory animals can disperse pathogens over long distances (Dingle, 2014; Pulgarín-R et al., 2019), or trigger infection outbreaks by exposing the population to pathogens in novel habitats (Lisovski et al., 2018; van Dijk et al., 2015). For example, migration of passerine birds has contributed to the spread of the West Nile Virus across North America (Owen et al., 2006), and the migration of waterfowl has contributed to the global spread of the highly pathogenic avian influenza (HPAI) H5N1 and H5N8 (Si et al., 2009; Xu et al., 2016).

Migration, however, can also reduce infection in a migratory population by so-called migration escape (Loehle, 1995; Satterfield et al., 2015). Migration allows hosts to 'escape' from the accumulated pathogens in the habitat. For example, Lesser black-backed gulls (*Larus fuscus*) with a relatively long migration distance have a lower seroprevalence of avian influenza virus (AIV) compared to those with a relatively short migration distance (Arriero et al., 2015). Previous studies that examined the interactions between bird migration and infection dynamics of pathogens focused on spatial–temporal and phylogenetic correlations between animal movements and infection outbreaks (Bourouiba

* Corresponding author at: Nanjing Normal University, Wenyuan Road 1, Nanjing 210046, China.
E-mail addresses: shenglai.yin@wur.nl (S. Yin), henjo.deknegt@wur.nl (H.J. de Knegt), mart.dejong@wur.nl (M.C.M. de Jong), yalisi@mail.tsinghua.edu.cn (Y. Si), herbert.prins@wur.nl (H.H.T. Prins), zhengyxhuang@gmail.com (Z.Y.X. Huang), fred.deboer@wur.nl (W.F. de Boer).

https://doi.org/10.1016/j.jtbi.2020.110315
0022-5193/

et al., 2010; Huang et al., 2019; Tian et al., 2015; Xu et al., 2016), whilst other aspects of migration that might affect infection prevalence have not yet been investigated, such as the configuration of the migration network and the synchrony in timing of migration.

Migratory animals, particularly migratory birds, can use stopover sites in a serial configuration, in which all individuals use the same stopover sites successively. The number of these stopover sites varies among species. For example, Sandpiper (*Calidris mauri*) and Black turnstone (*Arenaria melanocephala*) use stopover sites more frequently and spend less time to refuel on each site than Dunlin (*Calidris alpine*), Red knot (*C. canutus*) or Bar-tailed godwit (*Limosa lapponica*) (Iverson et al., 1996; Krementz et al., 2011; O'REILLY and Wingfield, 1995). On the other hand, migratory birds, such as Swan geese (*Anser cygnoides*), Bar-tailed godwits (*Limosa lapponica*), Brent geese (*Branta bernicla*) and Greater white-fronted geese (*Anser albifrons*) can use stopover sites in a parallel configuration (Batbayar et al., 2013; Battley et al., 2012; Green et al., 2002; Kölzsch et al., 2016), in which all individuals split to use multiple stopover sites at the same time. Hence, there are potentially many distinct network configurations with respect to the use of serial and parallel stopover sites. The configuration of a migration network is expected to influence the aggregation of migratory birds and their exposure to pathogens at these stopover sites (Buehler and Piersma, 2008; Rohani et al., 2009). Moreover, the increase in anthropogenic activities has decreased the availability of many stopover sites (Yamaguchi et al., 2008). For example, suitable stopover sites in the East Asian-Australian flyway have experienced a dramatic loss over the past 20 years, especially the stopover sites located in China (Jia et al., 2018; Zhang et al., 2015; Xu et al., 2019), which changes the configuration of migration networks. The effects of stopover sites loss on pathogen infection prevalence in a migratory population are not yet fully understood. To obtain a better understanding of infection dynamics in migratory populations and the spatio-temporal distribution of infection outbreaks, more studies are required that take into account the changes in network configurations of migratory species.

Apart from different configurations of migration network, migration synchrony (i.e., timing of migration) also varies among migratory species, due to e.g., differences in body condition, competition for limited resources, global warming, and optimization of mating opportunities (Morbey and Ydenberg, 2001; Muraoka et al., 2009). For example, a Swan goose population might only take weeks to leave a habitat, whereas a population of Barnacle geese might take months. Previous studies proposed that highly synchronized migration might be associated with high infection prevalence, as larger flocks lead to increased contact probabilities among individuals (Buehler and Piersma, 2008; Gaidet et al., 2011). However, no study has investigated how migration network configuration and migration synchrony affect the infection prevalence in a migratory goose population.

In this study, we applied a time-discrete SIR (susceptible-infected-recovered) model to various scenarios of spring migration to explore how variations in configuration of migration network and synchrony of migration affect infection prevalence. The model and scenarios were applied to infection of a low pathogenic avian influenza (LPAI) virus in migratory goose species, since the outbreaks of AIV caused concerns, but the relationship between goose migration and virus dispersal is not fully understood (Ren et al., 2016; Takekawa et al., 2010; Yin et al., 2017). We aimed at answering the following questions: (1) How does the configuration of a migration network affect infection prevalence? (2) Does highly synchronized timing of migration increase infection prevalence? (3) Is there a specific migration pattern, regarding the number of stopover sites and migration synchrony that minimizes pathogen infection?

2. Models

We first designed a simulation model that represents a migratory goose population (10,000 birds), then applied a SIR model to simulate the virus transmission during migration (Fig. 1). We included the environmental transmission process into the SIR model (Fig. 1), because the AIV can persist in the environment for an extended period, which can trigger a drastic virus accumulation, and significantly influence infection probability to geese (Ly et al., 2016).

Many studies suggested that models with frequency-dependent transmission can have a better fit to many wildlife disease data sets (de Jong et al., 1995; Dobson and Meagher, 1996; McCallum et al., 2001). For wild geese, they usually keep a certain distance between each other, the densities of the waterfowl on stopover sites was assumed to be constant. Moreover, a previous study suggested that a model integrating frequency-dependent transmission and environmental transmission had the best fitness to observed AIV infection prevalence (Roche et al., 2009). We therefore assumed that AIV transmission was frequency-dependent and independent of goose density.

To avoid the complex dynamics of infection and cross-immune responses to multiple virus strains, we modelled one goose population and a single AIV strain. As the antibodies to AIV within the geese can be detectable for a few months (Samuel et al., 2015), we assumed, following many previous modelling studies (Breban et al., 2009; Roche et al., 2009; Rohani et al., 2009), that migratory birds remained immune after recovery. We further assumed that migratory birds had no severe responses to the infection.

We simulate infection dynamics during the spring migration only; migratory goose species can play an important role in

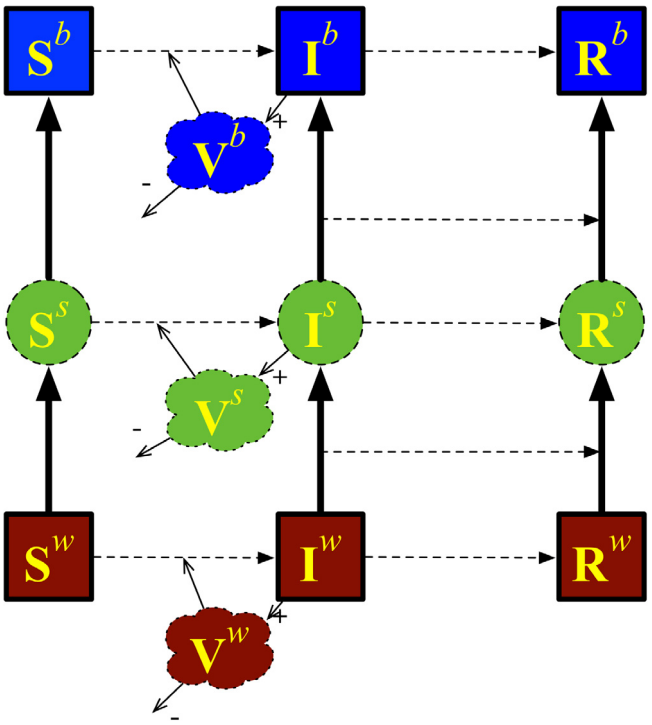

Fig. 1. Illustration of the SIR model. S, I, R are the susceptible, infected, recovered birds, and V is the virus in the environment. The dashed circles mean that the number of stopover sites varies in different scenarios. The superscript letters w, s, and b denote wintering ground, stopover sites, and breeding ground, respectively. The dashed lines denote the transition of the infectious status. The thick solid lines denote the movement of birds. The thin solid lines denote the dynamics of the virus in the environment.

dispersing AIV northwards (Xu et al., 2016), whilst it has been suggested that migratory goose species may not be exposed to AIV during their fall migration (Yin et al., 2017). Therefore, we only simulated spring migration. The simulations started with a virus-free population exposed to virus in their wintering grounds, and the simulation ended when all birds completed their migration.

2.1. Transmission dynamics on the ground

Virus transmission dynamics in wintering, stopover and breeding sites were simulated by using time-discrete SIR model. The number of susceptible birds (S), the number of infected birds (I), the number of recovered birds (R), and the total number of birds (N) was calculated in each site according to the following difference equations:

$$S_t^i = S_{t-1}^i - \frac{\beta S_{t-1}^i (I_{t-1}^i + \frac{V_{t-1}^i}{\varepsilon})}{N_{t-1}^i} - mo_{t-1}^i S_{t-1}^i + mi_{t-1}^{i-1} S_{t-1}^{i-1} \quad (1)$$

$$I_t^i = I_{t-1}^i + \frac{\beta S_{t-1}^i (I_{t-1}^i + \frac{V_{t-1}^i}{\varepsilon})}{N_{t-1}^i} - \gamma I_{t-1}^i - mo_{t-1}^i I_{t-1}^i + mi_{t-1}^{i-1} I_{t-1}^{i-1} \quad (2)$$

$$R_t^i = R_{t-1}^i + \gamma I_{t-1}^i - mo_{t-1}^i R_{t-1}^i + mi_{t-1}^{i-1} R_{t-1}^{i-1} \quad (3)$$

$$N_t^i = S_t^i + I_t^i + R_t^i \quad (4)$$

where β is the transmission rate parameter ($bird\ day^{-1}$), γ is the recovery probability (day^{-1}), m_{t-1}^i is the number of birds (bird) that migrate, V_t^i is the amount of virus in habitat i (see below), ε is the virus shedding rate (amount of virus shed per day per bird, $virus\ bird^{-1}\ day^{-1}$), t is the discrete time which was set as 0.1 day, and i is the site (i.e. a wintering, stopover, or breeding site). The proportions of migrating birds out or into site i are respectively mo and mi, such that mi always equals 0 for a wintering site, and mo always equals 0 for a breeding site.

The amount of virus in the environment (V_t^i) was calculated by the following difference equation:

$$V_t^i = V_{t-1}^i - \eta V_{t-1}^i + \varepsilon I_{t-1}^i - \eta \varepsilon I_{t-1}^i \quad (5)$$

where η is the virus decaying rate in the environment. We divided Eq. (5) by shedding rate ε ($virus\ bird^{-1}\ day^{-1}$) to obtain the following equation:

$$\frac{V_t^i}{\varepsilon} = \frac{V_{t-1}^i}{\varepsilon} - \eta \frac{V_{t-1}^i}{\varepsilon} + I_{t-1}^i - \eta I_{t-1}^i \quad (6)$$

which allows us to use v_t^i/ε ($bird$) to estimate the amount of virus in the environment (Rohani et al., 2009).

2.2. Infection dynamics during migration

In our time-discrete model, susceptible birds cannot be infected during flight due to absence of direct transmission or environmental transmission. Infected birds recover from infection and obtain immunity (Fig. 1).

Eqs. (7)–(10) depicted infection dynamics during the flight from site i to site j:

$$S_{t+\frac{\tau}{\omega}}^{ij} = m_t^i S_t^i \quad (7)$$

$$I_{t+\frac{\tau}{\omega}}^{ij} = m_t^i I_t^i (e^{-\gamma\tau/\omega}) \quad (8)$$

$$R_{t+\frac{\tau}{\omega}}^{ij} = m_t^i R_t^i + m_t^i I_t^i (1 - e^{-\gamma\tau/\omega}) \quad (9)$$

$$\tau = \frac{d}{v} \quad (10)$$

ω is the number of stops in the migration network, τ is the total number of flying days (day) from wintering to breeding ground, d is the total migration distance (km), and v is the averaged flying speed ($km\ day^{-1}$).

2.3. Migration patterns

We designed three different configurations of the migration network, networks with serial stopover sites (Fig. 2, network S), networks with parallel stopover sites (Fig. 2, network P), and networks with both serial and parallel stopover sites (Fig. 2, network PSS, SPS and SSP). In the parallel configurations, birds distributed evenly over all stopover sites.

Field observations showed that the arrival and departure of waterfowl generally follow a unimodal pattern (Gupta et al., 2010; van Gils et al., 2007). Therefore, we used a truncated Gaussian distribution to calculate the proportion of individuals that migrate at each time step t (mi and mo):

$$m_t^i = \begin{cases} \int_t^{t+1} N(\mu^i, \sigma^2) \times \frac{1}{\int_{\mu^i-3\sigma}^{\mu^i+3\sigma} N(\mu^i, \sigma^2)}, & \mu^i - 3\sigma \le t \le \mu^i + 3\sigma \\ 0, & else \end{cases} \quad (11)$$

where μ^i is the mean day of the migration departure date from habitat i, σ is the spread of the distribution around the mean. As can be seen from the truncation, we assumed that the whole population departs from (and arrive at) a site within 6σ days. Therefore, the migration synchrony can be increased or decreased by changing the parameter 6σ. A greater 6σ represents a lower synchrony of migration, and *vice versa*.

We used the unimodal, truncated Gaussian distribution as it is more close to the patterns observed in nature. However, we could easily apply other distributions to simulate the waterfowl migration pattern. For example, distribution with a constant migration proportion, which gives a higher synchrony than a truncated Gaussian distribution, generated a similar pattern in the results, but the accumulative infection was a little lower than those obtained from a truncated Gaussian distribution.

2.4. Model parameterisation

The recovery rate γ was set as 0.1 according to a previous study suggesting that the median infectious period for LPAI infected ducks was 10–11.5 days (Hénaux and Samuel, 2011). The transmission rate (β) of AIV is largely unknown, especially for wild populations (Lisovski et al., 2018), and we therefore used the value 0.05, 0.1 and 0.2, which translates to a basic reproduction number, R_0, from 0.5 to 2. Different values of β generated qualitatively similar results (Fig. S1), thus we here only reported the results from simulations with β = 0.1 (R_0 = 1).

The AIV can persist in water for an extended period, and the persistence of AIV ranges between days to a couple of weeks, depending on temperature and pH (Brown et al., 2009). We set the virus decaying rate (η) at 0.03, following previous studies (Roche et al., 2009; Rohani et al., 2009). As migratory birds share stopover sites in their migration (Brown et al., 2009; Stallknecht et al., 1990), we assumed, following a previous study (Breban et al., 2009), that the stopover sites were contaminated at a low level (V_i^0 / ε = 365 bird days) before arrival of the migratory birds. In addition, a previous study showed that white-fronted geese (*A. albifrons*) take 83 days for spring migration with a travel time of 23 days (Kölzsch et al., 2016), we thus set the total refuelling time (T) at 60 days. The parameters and references were listed in Table 1.

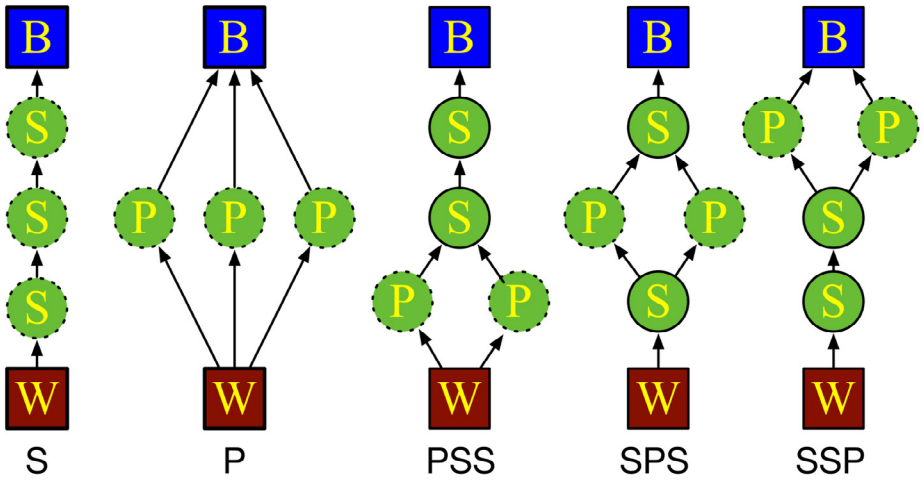

Fig. 2. Illustrations of different migration networks with serial stopover sites (S), parallel stopover sites (P), and serial-parallel stopover sites. PSS network has the earliest parallel stopover sites and SSP has the latest parallel stopover sites in the network. The wintering ground, stopover sites, and breeding ground are depicted in red, green, and blue, respectively. The dashed circles mean that the number of stopover sites varies in different scenarios. (2-column). (For interpretation of the references to colour in this figure legend, the reader is referred to the web version of this article.)

Table 1
The parameters of the model with their definitions, used values, and references.

Parameter	Definition	Used values	references
N_0	population size	10,000 bird	–
β	transmission rate	0.1 bird day^{-1}	–
γ	recovery rate probability	0.1 day^{-1}	(Hénaux and Samuel, 2011)
6σ	length of the migration synchrony	0–13 week	–
η	virus decaying rate in the environment	0.03 day^{-1}	(Brown et al., 2009)
d	migration distance	3900 km	(Kölzsch et al., 2016)
v	flying speed	1680 km/day	(Kölzsch et al., 2016)
τ	total flying days	2.32 days	
ω	number of stops	0–10	–
V_i^0 / ε	initial amount of virus in the amount of virus shed per infectious bird	365 bird days	(Breban et al., 2009)
T	total refuelling days	60 days	(Kölzsch et al., 2016)

2.5. Model analyses

To examine whether there is an optimal migration pattern that minimizes infection prevalence, we combined various migration networks and various levels of migration synchrony (6σ = 0, 1, 2...13). Since the migration synchrony influences the abundance of birds on successive stopover sites, we only considered the migration networks with serial stopover sites (number of stopover site = 0, 1, 2, 3... 10). In total, we evaluated 154 scenarios with different combinations of numbers of serial stopover sites and different levels of migration synchrony to test for their impacts on infection prevalence. During simulation, all other variables were kept constant. To compare the differences in virus transmission among scenarios, we calculated the average number of cumulative infection during the infection period of each scenario. All models were constructed and analysed in R 3.6.1.

3. Results

3.1. Effect of migration network configuration on infection

In networks with only serial stopover sites, environmental transmission contributed more than 70% to the total infection prevalence. However, its contribution decreased along the increasing number of serial stopover sites (Fig. 3), and this pattern did not change qualitatively when the transmission rate (β) and the initial virus in the environment (V_i^0 / ε) vary (Fig. S1). An increasing number of sites also reduced both the cumulative infection (i.e. sum of recovered birds and infected birds) and the peak value of infection

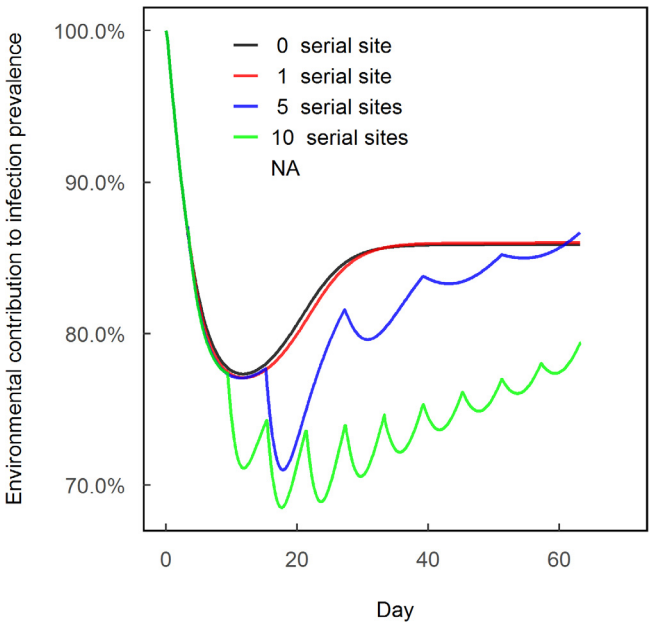

Fig. 3. Simulated environmental contributions to the total prevalence of infection. The moment of arrival at a stopover site is visible in the graph by a sudden sharp drop in environmental contribution. These results are obtained from migration networks with 0, 1, 5, and 10 serial stopover sites. All birds migrate at the same time (6σ = 0).

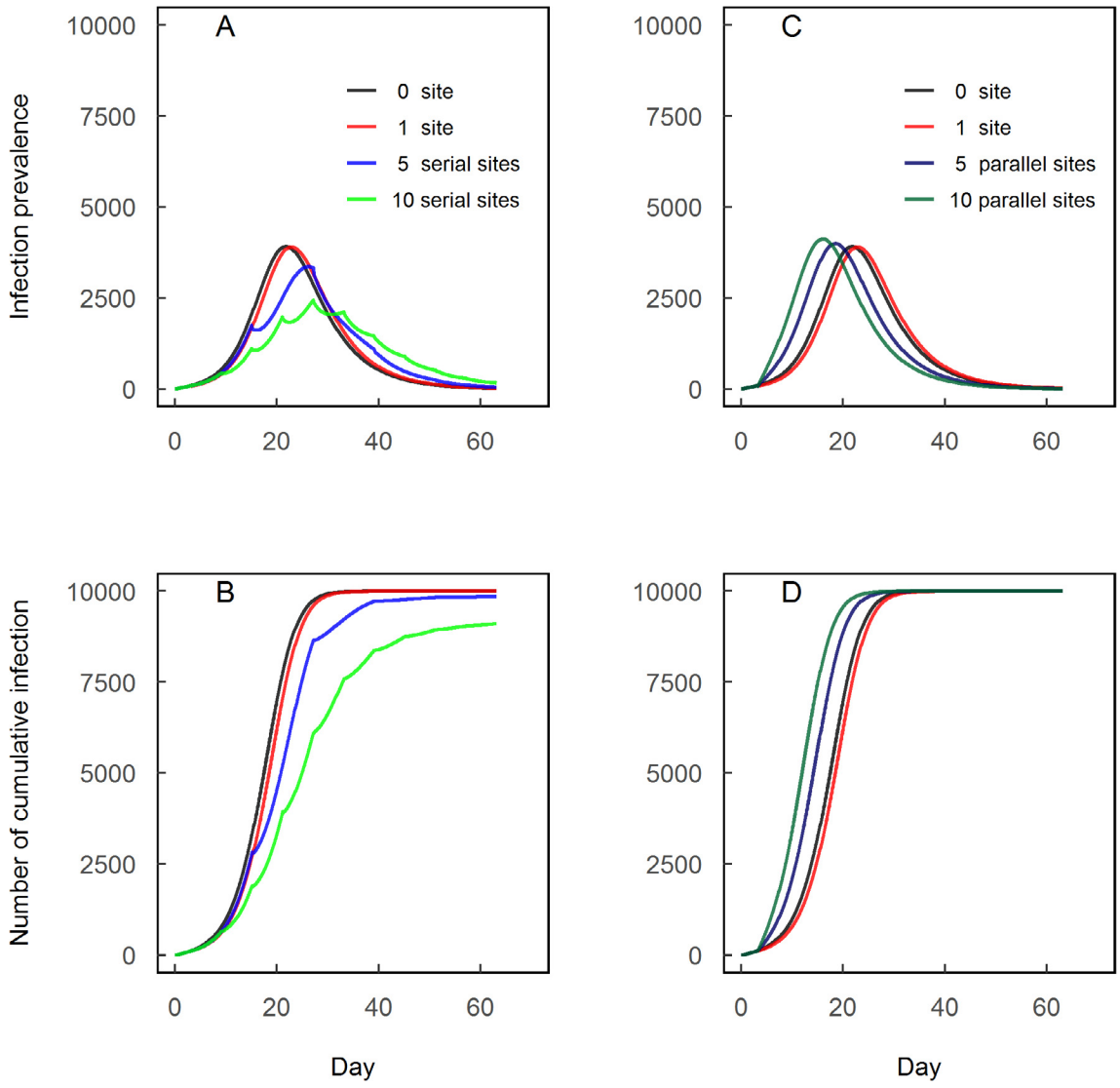

Fig. 4. Simulated prevalence of infection (A, C) and prevalence of cumulative infection (B, D). These results are obtained from migration networks with 0, 1, 5 and 10 serial stopover sites (A, B), and with 5, 10 parallel stopover sites (C, D). All birds migrate at the same time ($6\sigma = 0$).

prevalence in the migratory population (Fig. 4A and B). The infection prevalence in the second half of the migration period was higher under an increasing number of stopover sites. This because most birds were already recovered in simulations with less stopover sites, and hence, more susceptible birds could be infected in simulation with more stopover sites in this second half of the migration period.

In networks with parallel sites, both an increasing number of parallel sites and earlier use of parallel stopover sites during migration led to a faster accumulation of infections, and therefore, an earlier infection peak in the migratory population (Fig. 4C and D, and Fig. 5). Similar patterns were observed when we varied the initial amount of virus in the environment.

3.2. Effect of migration synchrony on infection

Expanding migration synchrony led to an increase in the number of cumulative infections and the average number of cumulative infection (Figs. 6 and 7). A migration pattern with multiple serial stopover sites (n = 10) and highly synchronized migration ($6\sigma = 0$) led to the lowest average number of cumulative infections. The effect of migration synchrony on the average number of cumulative infections interacted with the effect of the number of stopover sites, because the number of serial stopover sites had the largest effect when migration was the most synchronized (Fig. 7).

4. Discussion

In our simulation, we found that the configuration of the migration network and the synchrony in timing of migration affected the infection dynamics in a migratory population. Specifically, we found that migration can reduce the infection prevalence in the population, which is in agreement with migratory escape (Loehle, 1995; Satterfield et al., 2015). Furthermore, synchronized migration did not increase infection prevalence, but in contrast, reducing migration synchrony led to an increasing average number of cumulative infection.

Since AIV accumulate in the environment and can persist for weeks or even months (Hénaux and Samuel, 2011; Stallknecht et al., 1990), staying in a single habitat for a long period increases the risks for infection with the virus in the environment. This is also illustrated by the fact that infection prevalence in resident

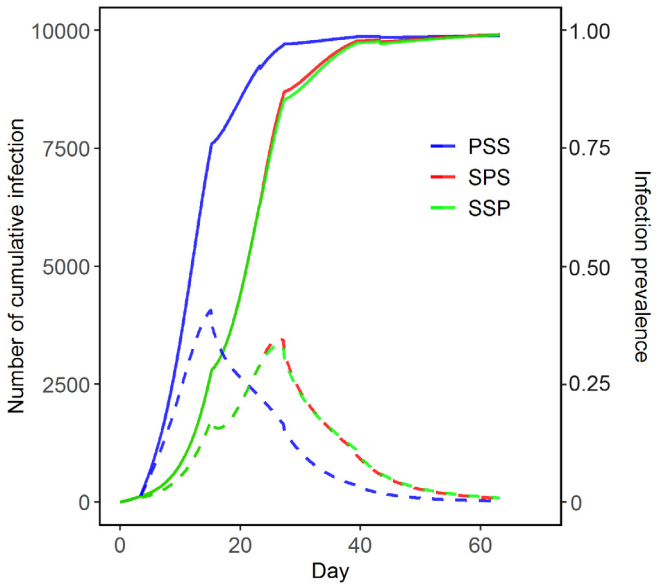

Fig. 5. Simulated infection prevalence (dashed lines) and number of cumulative infection (solid lines). These results are obtained from migration networks that contain 1 pair of parallel stopover sites and 2 serial stopover sites. The position of P in the legend indicates the positions of the parallel stopover sites in the migration networks. All birds migrate at the same time ($6\sigma = 0$).

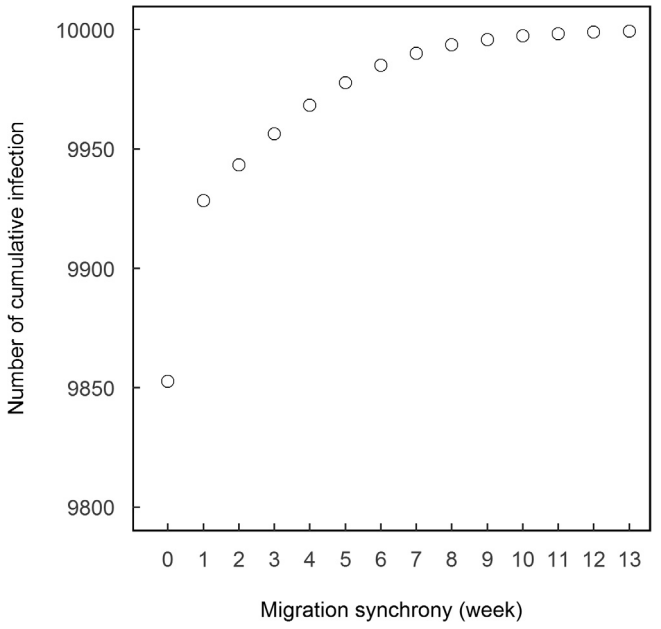

Fig. 6. Number of cumulative infection at the end of migration. These results are obtained from migration networks with 5 serial stopover sites, and with various levels of migration synchrony (6σ = 1,2,3. . . . .13).

waterfowl can be year-round (Newman et al., 2009), but the infection prevalence in migratory waterfowl can be extremely low over its annual lifecycle (Newman et al., 2009; Yin et al., 2017).

Although our model assumes one virus strain and permanent immunity from infection, the results further indicate that migratory hosts can reduce their infection prevalence by stopping on stopover sites in a serial configuration. This is because, when migratory geese start arriving at a new site that has a very low accumulation of virus in the environment, environmental transmission contributes relatively little to the force of infection. This is in line with the concept of migratory escape (Altizer et al., 2011; Loehle, 1995), which is also supported by empirical studies. For example, in reindeer (*Rangifer tarandus*) herds, migration can significantly reduce the abundance of the parasitic warble fly larvae (*Hypoderma tarandi*) in the population (Folstad et al., 1991).

On the contrary, parallel stopover sites increased infection prevalence. Although the use of parallel stopover sites reduced the abundance of migratory geese in each stopover site, it did not influence the direct transmission probability in our density-independent transmission model. However, when the migratory population used parallel stopover sites, especially at the early stage of the migration, it was exposed to larger total amount of virus that existed in the environment, which sped-up the accumulation of infections. The fast accumulation of infections that was associated with earlier parallel sites in the migration network (Fig. 3) might contribute to an absence of AIV infection in migratory geese later on (Yin et al., 2017). For example, Greater white-fronted geese use multiple parallel stopover sites in the early stages of their spring migration (Kölzsch et al., 2016), which might increase infection prevalence so fast that the majority of the population might have recovered from their infection later on. Thereby, the Greater white-fronted geese might not be able to introduce the pathogen to their breeding ground. Many other migratory species, such as Snow geese (*Anser caerulescens*), Sandhill cranes (*Antigone Canadensis*) and Demoiselle cranes (*Grus virgo*), also use stopover sites in a parallel configuration (Prins and Namgail, 2017; Samuel et al., 2015). We predict that, in these species, infection peaks at an earlier stage of their migration than that of similar species with a relatively unidirectional migration, such as Barnacle geese (Eichhorn et al., 2006; Shariatinajafabadi et al., 2014). To test this prediction, we are calling for more empirical studies, involving outbreak monitoring and GPS tracking of bird migration.

Previous studies have suggested that animal movements in large flocks might facilitate infection prevalence, and cause outbreaks due to more frequent contact among animals in dense aggregations (Altizer et al., 2011). This idea does not hold in our simulation since we assumed that, in migratory goose population, the transmission of AIV was density-independent. However, our simulation showed that a larger migrating flock with synchronized migration can negatively affect infection prevalence, because when the geese migrated with a synchronized pattern (i.e., $6\sigma = 0$), they experienced a low infection risk at each new stopover sites due to the lower amount of viruses present in the environment. However, when the geese migrate with an expanding migration synchrony (e.g., $6\sigma = 13$), they experienced a high infection risk because the amount of viruses in the environment had been elevated by infected birds that arrived earlier.

Migratory waterfowl have distinct migration patterns in terms of number of stopover site and migration synchrony. For example, Swan geese (*Anser cygnoides*) migrate over about 13 stopover sites with a relatively synchronized migration in about 5 weeks (Batbayar et al., 2013), Mallard (*Anas platyrhynchos*) use about 3 stopover sites with a relatively synchronized migration in about 5–7 weeks (Yamaguchi et al., 2008), whereas Barnacle geese often only use a single stopover site (Tombre et al., 2008) with an extremely expanded migration synchrony in about 4 months (Hornman et al., 2015). Our simulations showed that the migration pattern influenced infection dynamics, and that multiple serial stopover sites with high migration synchrony minimized the average number of cumulative infections (Fig. 5). Our study indicates that a specific combination of the migration network configuration and migration synchrony can minimize transmission of AIV during migration.

Our results showed that the migration network configuration and migration synchrony affect pathogen infection prevalence in a migratory population by influencing the amount of viruses that is encountered by the migratory population. Therefore, the environ-

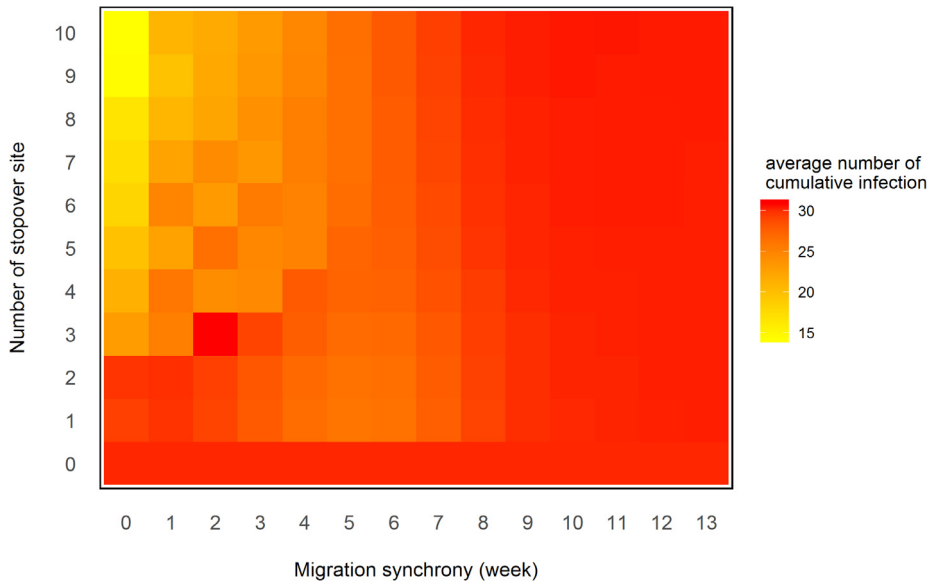

Fig. 7. Average number of cumulative infections during the whole migration period. Results are obtained from various migration patterns that vary in number of serial stopover sites (n = 0, 1, 2, 3…10) and timing of migration synchrony (6σ = 1,2,3……13).

mental transmission determines the infection dynamics, which is consistent with previous modelling studies (Breban et al., 2009; Hénaux and Samuel, 2011; Rohani et al., 2009). Studies that examined the role of environmental transmission investigated the effects of varying virus decaying rates in different seasons (Breban et al., 2009). In our study, since we only simulated a single-season migration, we applied a constant virus decaying rate for examining the effects of network configuration and migration synchrony. Since the effects of network configuration and migration synchrony depends on the amounts of viruses in the environment, we expect that their effects are correlated with the virus decaying rate. For example, ambient temperature is positively correlated with the virus decaying rate (Stallknecht et al., 1990), and therefore, effects of network configuration and migration synchrony can be reduced under warmer temperature scenarios or at relatively lower latitudes.

Although the importance of environmental transmission has been addressed by both modelling (Breban et al., 2009; Rohani et al., 2009) and empirical studies (de Rueda et al., 2015; Gaidet et al., 2010; Ly et al., 2016), very few efforts have been devoted to environmental monitoring. However, it is necessary to perform environmental monitoring in critical sites that are intensively used by multiple migratory waterfowl species during seasonal migration, and that are hotspots for AIV outbreaks.

We assumed a constant population size in a single spring migration. In multiple-season migrations, however, population sizes vary from year to year. Although population size did not affect the infection probability via direct transmission in our model, it may positively affect infection prevalence by increasing the accumulation of virus in the environment. Furthermore, we only simulated spring migration as we aimed to study how the AIV infection dispersed to the North by geese under influence of various migration network configurations. Modelling autumn migration, when there are many young birds, requires to also include the population's age structure into the model, as young birds are naive, and therefore more susceptible to AIV infection. Further modelling studies that focus on animal migration and pathogen infection prevalence can address these aspects by taking into account the dynamics in population demography.

In general, our simulations demonstrate that migration patterns can affect infection dynamics in a migratory population. Although our study focused on a system with single AIV strain and only one migratory geese population, the findings can be extended to other migratory host species, and other pathogens that can persist in the environment. As availability of suitable stopover sites is threatened by human activities (Xu et al., 2019), we call for more studies that analyse the effects of network configuration, timing of migration (e.g., under influence of global climate change), and movement patterns on disease dynamics. Application of mathematical modelling of animal movements over a migration network can be greatly helpful in understanding mechanisms related to pathogen dispersal.

CRediT authorship contribution statement

Shenglai Yin: Conceptualization, Formal analysis, Funding acquisition, Methodology, Writing - original draft. **Henrik J. Knegt:** Formal analysis, Methodology. **Mart C.M. Jong:** Conceptualization, Methodology, Writing - review & editing. **Yali Si:** . **Herbert H.T. Prins:** Conceptualization, Supervision, Writing - review & editing. **Zheng Y.X. Huang:** Conceptualization, Formal analysis, Funding acquisition, Writing - review & editing. **Willem F. Boer:** Conceptualization, Supervision, Writing - review & editing.

Declaration of Competing Interest

The authors declare that they have no known competing financial interests or personal relationships that could have appeared to influence the work reported in this paper.

Acknowledgments

We thank Yanjie Xu and Joost de Jong at Wageningen University for their feedback on this work.

Funding

Z.Y.X. Huang is supported by the National Natural Science Foundation of China (31870400). S.Yin is supported by the Chinese Scholarship Council (201406190178).

Appendix A. Supplementary data

Supplementary data to this article can be found online at https://doi.org/10.1016/j.jtbi.2020.110315.

References

Altizer, S., Bartel, R., Han, B.A., 2011. Animal migration and infectious disease risk. Science 331, 296–302.

Arriero, E., Müller, I., Juvaste, R., Martínez, F.J., Bertolero, A., 2015. Variation in immune parameters and disease prevalence among lesser black-backed gulls (Larus fuscus sp.) with different migratory strategies. PLoS ONE 10, e0118279.

Batbayar, N., Takekawa, J.Y., Newman, S.H., Prosser, D.J., Natsagdorj, T., Xiao, X., 2013. Migration strategies of Swan Geese Anser cygnoides from northeast Mongolia. Wildfowl 61, 90–109.

Battley, P.F., Warnock, N., Tibbitts, T.L., Gill Jr, R.E., Piersma, T., Hassell, C.J., Douglas, D.C., Mulcahy, D.M., Gartrell, B.D., Schuckard, R., 2012. Contrasting extreme long-distance migration patterns in bar-tailed godwits Limosa lapponica. J. Avian Biol. 43, 21–32.

Bourouiba, L., Wu, J., Newman, S., Takekawa, J., Natdorj, T., Batbayar, N., Bishop, C. M., Hawkes, L.A., Butler, P.J., Wikelski, M., 2010. Spatial dynamics of bar-headed geese migration in the context of H5N1. J. R. Soc. Interface 7, 1627–1639. https://doi.org/10.1098/rsif.2010.0126.

Breban, R., Drake, J.M., Stallknecht, D.E., Rohani, P., 2009. The role of environmental transmission in recurrent avian influenza epidemics. PLoS Comput. Biol. 5, e1000346.

Brown, J.D., Goekjian, G., Poulson, R., Valeika, S., Stallknecht, D.E., 2009. Avian influenza virus in water: infectivity is dependent on pH, salinity and temperature. Vet. Microbiol. 136, 20–26.

Buehler, D.M., Piersma, T., 2008. Travelling on a budget: Predictions and ecological evidence for bottlenecks in the annual cycle of long-distance migrants. Phil. Trans. R. Soc. B 363, 247–266.

de Jong, M. C. M., Diekmann, O., Heesterbeek, H., 1995. How does transmission of infection depend on population size? . In: Mollison, D., (Ed.), Epidemic Models. Cambridge University Press, Cambridge, pp. 84–94.

de Rueda, C.B., de Jong, M.C., Eblé, P.L., Dekker, A., 2015. Quantification of transmission of foot-and-mouth disease virus caused by an environment contaminated with secretions and excretions from infected calves. Vet. Res. 46, 43.

Dingle, H., 2014. Migration: the Biology of Life on the Move. Oxford University Press, USA.

Dobson, A., Meagher, M., 1996. The population dynamics of brucellosis in the Yellowstone National Park. Ecology 77, 1026–1036.

Eichhorn, G., Afanasyev, V., Drent, R.H., van der Jeugd, H.P., 2006. Spring stopover routines in Russian Barnacle Geese Branta leucopsis tracked by resightings and geolocation. Ardea 94, 667.

Folstad, I., Nilssen, A.C., Halvorsen, O., Andersen, J., 1991. Parasite avoidance: the cause of post-calving migrations in Rangifer? Can. J. Zool. 69, 2423–2429.

Gaidet, N., Cappelle, J., Takekawa, J.Y., Prosser, D.J., Iverson, S.A., Douglas, D.C., Perry, W.M., Mundkur, T., Newman, S.H., 2010. Potential spread of highly pathogenic avian influenza H5N1 by wildfowl: dispersal ranges and rates determined from large-scale satellite telemetry. J. Appl. Ecol. 47, 1147–1157.

Gaidet, N., Caron, A., Cappelle, J., Cumming, G.S., Balança, G., Hammoumi, S., Cattoli, G., Abolnik, C., Servan de Almeida, R., Gil, P., 2011. Understanding the ecological drivers of avian influenza virus infection in wildfowl: a continental-scale study across Africa. Proc. R. Soc. B. 279, 1131–1141.

Green, M., Alerstam, T., Clausen, P., Drent, R., Ebbinge, B.S., 2002. Dark-bellied Brent Geese Branta bernicla bernicla, as recorded by satellite telemetry, do not minimize flight distance during spring migration. Ibis 144, 106–121.

Gupta, R.C., Kaushik, T.K., Surjit, K., 2010. An account concerning arrival and departure time of few selected winter migratory birds in Haryana rural ponds. Environ. Conserv. J. 11, 1–9.

Hénaux, V., Samuel, M.D., 2011. Avian influenza shedding patterns in waterfowl: implications for surveillance, environmental transmission, and disease spread. J. Wildlife. Dis. 47, 566–578.

Hornman, M., Hustings, F., Koffijberg, K., Klaassen, O., Kleefstra, R., van Winden, E., 2015. Watervogels in Nederland in 2012/2013. SOVON monitoring report, Vol. 1.

Huang, Z.Y.X., Xu, C., van Langevelde, F., Ma, Y., Langendoen, T., Mundkur, T., Si, Y., Tian, H., Kraus, R.H.S., Gilbert, M., Han, G.-Z., Ji, X., Prins, H.H.T., de Boer, W.F., 2019. Contrasting effects of host species and phylogenetic diversity on the occurrence of HPAI H5N1 in European wild birds. J. Anim. Ecol. 88, 1044–1053.

Iverson, G.C., Warnock, S.E., Butler, R.W., Bishop, M.A., Warnock, N., 1996. Spring migration of western sandpipers along the Pacific coast of North America: a telemetry study. Condor 98, 10–21.

Jia, Q., Wang, X., Zhang, Y., Cao, L., Fox, A.D., 2018. Drivers of waterbird communities and their declines on Yangtze River floodplain lakes. Biol. Conserv. 218, 240–246.

Kölzsch, A., Müskens, G.J., Kruckenberg, H., Glazov, P., Weinzierl, R., Nolet, B.A., Wikelski, M., 2016. Towards a new understanding of migration timing: slower spring than autumn migration in geese reflects different decision rules for stopover use and departure. Oikos 125, 1496–1507.

Krementz, D.G., Asante, K., Naylor, L.W., 2011. Spring migration of mallards from Arkansas as determined by satellite telemetry. J. Fish. Wildl. Manag. 2, 156–168.

Lisovski, S., van Dijk, J.G., Klinkenberg, D., Nolet, B.A., Fouchier, R.A., Klaassen, M., 2018. The roles of migratory and resident birds in local avian influenza infection dynamics. J. Appl. Ecol. 55, 2963–2975.

Loehle, C., 1995. Social barriers to pathogen transmission in wild animal populations. Ecology 76, 326–335.

Ly, S., Vong, S., Cavailler, P., Mumford, E., Mey, C., Rith, S., Van Kerkhove, M.D., Sorn, S., Sok, T., Tarantola, A., 2016. Environmental contamination and risk factors for transmission of highly pathogenic avian influenza A (H5N1) to humans, Cambodia, 2006–2010. BMC Infect. Dis. 16, 631.

McCallum, H., Barlow, N., Hone, J., 2001. How should pathogen transmission be modelled? Trends Ecol. Evol. 16, 295–300.

Morbey, Y.E., Ydenberg, R.C., 2001. Protandrous arrival timing to breeding areas: a review. Ecol. Lett. 4, 663–673.

Muraoka, Y., Schulze, C.H., Pavličev, M., Wichmann, G., 2009. Spring migration dynamics and sex-specific patterns in stopover strategy in the Wood Sandpiper Tringa glareola. J. Ornithol. 150, 313–319.

Newman, S.H., Iverson, S.A., Takekawa, J.Y., Gilbert, M., Prosser, D.J., Batbayar, N., Natsagdorj, T., Douglas, D.C., 2009. Migration of whooper swans and outbreaks of highly pathogenic avian influenza H5N1 virus in eastern Asia. PLoS ONE 4, e5729.

O'reilly, K.M., Wingfield, J.C., 1995. Spring and autumn migration in Arctic shorebirds: same distance, different strategies. Am. Zool. 35, 222–233.

Owen, J., Moore, F., Panella, N., Edwards, E., Bru, R., Hughes, M., Komar, N., 2006. Migrating birds as dispersal vehicles for West Nile virus. EcoHealth 3, 79.

Prins, H.H., Namgail, T., 2017. Bird Migration Across the Himalayas: Wetland Functioning Amidst Mountains and Glaciers. Cambridge University Press, Cambridge.

Pulgarín-R, P.C., Gómez, C., Bayly, N.J., Bensch, S., Cadena, C.D., 2019. Migratory birds as vehicles for parasite dispersal? Infection by avian haemosporidians over the year and throughout the range of a long-distance migrant. J. Biogeogr. 46, 83–96.

Ren, H., Jin, Y., Hu, M., Zhou, J., Song, T., Huang, Z., Li, B., Li, K., Zhou, W., Dai, H., 2016. Ecological dynamics of influenza A viruses: cross-species transmission and global migration. Sci. Rep. 6, 36839.

Roche, B., Lebarbenchon, C., Gauthier-Clerc, M., Chang, C.-M., Thomas, F., Renaud, F., Van Der Werf, S., Guegan, J.-F., 2009. Water-borne transmission drives avian influenza dynamics in wild birds: the case of the 2005–2006 epidemics in the Camargue area. Infect. Genet. Evol. 9, 800–805.

Rohani, P., Breban, R., Stallknecht, D.E., Drake, J.M., 2009. Environmental transmission of low pathogenicity avian influenza viruses and its implications for pathogen invasion. Proc. Natl. Acad. Sci. USA 106, 10365–10369.

Samuel, M.D., Hall, J.S., Brown, J.D., Goldberg, D.R., Ip, H., Baranyuk, V.V., 2015. The dynamics of avian influenza in Lesser Snow Geese: implications for annual and migratory infection patterns. Ecol. Appl. 25, 1851–1859.

Satterfield, D.A., Maerz, J.C., Altizer, S., 2015. Loss of migratory behaviour increases infection risk for a butterfly host. Proc. R. Soc. B. 282, 20141734.

Shariatinajafabadi, M., Wang, T., Skidmore, A.K., Toxopeus, A.G., Kölzsch, A., Nolet, B. A., Exo, K.-M., Griffin, L., Stahl, J., Cabot, D., 2014. Migratory herbivorous waterfowl track satellite-derived green wave index. PLoS ONE 9, e108331.

Si, Y., Skidmore, A.K., Wang, T., de Boer, W.F., Debba, P., Toxopeus, A.G., Li, L., Prins, H.H., 2009. Spatio-temporal dynamics of global H5N1 outbreaks match bird migration patterns. Geospatial. Health 4, 65–78.

Stallknecht, D., Kearney, M., Shane, S., Zwank, P., 1990. Effects of pH, temperature, and salinity on persistence of avian influenza viruses in water. Avian Dis., 412–418

Takekawa, J.Y., Prosser, D.J., Newman, S.H., Muzaffar, S.B., Hill, N.J., Yan, B., Xiao, X., Lei, F., Li, T., Schwarzbach, S.E., 2010. Victims and vectors: highly pathogenic avian influenza H5N1 and the ecology of wild birds. Avian Biol. Res. 3, 51–73.

Tian, H., Zhou, S., Dong, L., Van Boeckel, T.P., Cui, Y., Newman, S.H., Takekawa, J.Y., Prosser, D.J., Xiao, X., Wu, Y., 2015. Avian influenza H5N1 viral and bird migration networks in Asia. Proc. Natl. Acad. Sci. USA 112, 172–177.

Tombre, I.M., Høgda, K.A., Madsen, J., Griffin, L.R., Kuijken, E., Shimmings, P., Rees, E., Verscheure, C., 2008. The onset of spring and timing of migration in two arctic nesting goose populations: the pink-footed goose Anser bachyrhynchus and the barnacle goose Branta leucopsis. J. Avian Biol. 39, 691–703.

van Dijk, J.G., Fouchier, R.A., Klaassen, M., Matson, K.D., 2015. Minor differences in body condition and immune status between avian influenza virus-infected and noninfected mallards: a sign of coevolution?. Ecol. Evol. 5, 436–449.

van Gils, J.A., Munster, V.J., Radersma, R., Liefhebber, D., Fouchier, R.A., Klaassen, M., 2007. Hampered foraging and migratory performance in swans infected with low-pathogenic avian influenza A virus. PLoS ONE 2, e184.

Xu, Y., Gong, P., Wielstra, B., Si, Y., 2016. Southward autumn migration of waterfowl facilitates cross-continental transmission of the highly pathogenic avian influenza H5N1 virus. Sci. Rep. 6, 30262.

Xu, Y., Si, Y., Wang, Y., Zhang, Y., Prins, H.H.T., Cao, L., de Boer, W.F., 2019. Loss of functional connectivity in migration networks induces population decline in migratory birds. Ecol. Appl. 29, e01960.

Yamaguchi, N., Hiraoka, E., Fujita, M., Hijikata, N., Ueta, M., Takagi, K., Konno, S., Okuyama, M., Watanabe, Y., Osa, Y., 2008. Spring migration routes of mallards (Anas platyrhynchos) that winter in Japan, determined from satellite telemetry. Zool. Sci. 25, 875–882.

Yin, S., Kleijn, D., Müskens, G.J., Fouchier, R.A., Verhagen, J.H., Glazov, P.M., Si, Y., Prins, H.H., de Boer, W.F., 2017. No evidence that migratory geese disperse avian influenza viruses from breeding to wintering ground. PLoS ONE 12, e0177790.

Zhang, Y., Jia, Q., Prins, H.H.T., Cao, L., de Boer, W.F., 2015. Effect of conservation efforts and ecological variables on waterbird population sizes in wetlands of the Yangtze River. Sci. Rep. 5, 17136.